

Infrared Small Target Detection based on Adjustable Sensitivity Strategy and Multi-Scale Fusion

Zhao Jinmiao^{1,2,3,4}, Shi Zelin^{1,2,*}, Yu Chuang^{1,2,3,4}, and Liu Yunpeng^{1,2}

¹Key Laboratory of Opto-Electronic Information Processing, Chinese Academy of Sciences

²Shenyang Institute of Automation, Chinese Academy of Sciences

³Institutes for Robotics and Intelligent Manufacturing, Chinese Academy of Sciences

⁴University of Chinese Academy of Sciences

Abstract. Recently, deep learning-based single-frame infrared small target (SIRST) detection technology has made significant progress. However, existing infrared small target detection methods are often optimized for a fixed image resolution, a single wavelength, or a specific imaging system, limiting their breadth and flexibility in practical applications. Therefore, we propose a refined infrared small target detection scheme based on an adjustable sensitivity (AS) strategy and multi-scale fusion. Specifically, a multi-scale model fusion framework based on multi-scale direction-aware network (MSDA-Net) is constructed, which uses input images of multiple scales to train multiple models and fuses them. Multi-scale fusion helps characterize the shape, edge, and texture features of the target from different scales, making the model more accurate and reliable in locating the target. At the same time, we fully consider the characteristics of the infrared small target detection task and construct an edge enhancement difficulty mining (EEDM) loss. The EEDM loss helps alleviate the problem of category imbalance and guides the network to pay more attention to difficult target areas and edge features during training. In addition, we propose an adjustable sensitivity strategy for post-processing. This strategy significantly improves the detection rate of infrared small targets while ensuring segmentation accuracy. Extensive experimental results show that the proposed scheme achieves the best performance. Notably, this scheme won the first prize in the PRCV 2024 wide-area infrared small target detection competition.

Keywords: Infrared small target detection, Multi-scale fusion, Adjustable sensitivity strategy, Edge enhancement difficulty mining loss.

1 Introduction

With the continuous maturity of infrared imaging detection technology, infrared small target detection has been widely used in many fields, such as target recognition and tracking, satellite monitoring, and earthquake rescue [1]. Currently, existing methods based on infrared small target detection are often applicable to fixed image resolution, single wavelength or specific imaging systems, which limits their breadth and flexibility in practical applications. Therefore, constructing an infrared small

target detection scheme suitable for multiple resolutions, multiple wavelengths and multiple scenes is challenging.

The research on infrared small target detection can be divided into non-deep learning-based methods and deep learning-based methods. Non-deep learning-based infrared small target detection methods mainly use the characteristics of infrared small target images for detection [2-4]. These methods are usually designed for specific scenarios and perform well under certain conditions. However, owing to the complexity and variability of real-world scenarios, these traditional methods often suffer from many false detections or even failure. To solve these problems and consider the powerful feature extraction capabilities of convolutional neural networks, deep learning-based methods [5-7] have been widely studied. In recent years, deep learning-based infrared small target detection methods have made significant progress. However, existing deep learning-based infrared small target detection methods are often optimized for a fixed image resolution, a single wavelength, or a specific imaging system, which limits their breadth and flexibility in practical applications.

To solve this problem, we construct a refined infrared small target detection scheme based on an adjustable sensitivity strategy and multi-scale fusion. First, considering the powerful learning ability of deep learning-based methods, we explore multiple excellent infrared small target detection networks and select MSDA-Net [8] as our backbone network. At the same time, considering the multi-scale challenges of dataset samples, we train and select multi-scale models and reasonably integrate the results of multiple models to achieve more accurate segmentation. In addition, to alleviate the problem of class imbalance and guide the network to pay more attention to difficult samples and edge features during training, we propose an edge enhancement difficulty mining (EEDM) loss. This loss helps the model learn valuable features more effectively and greatly avoids the risk of small targets being submerged by the background. In addition, to further improve the overall performance of the proposed method, we propose an adjustable sensitivity (AS) strategy for post-processing. This strategy introduces the concepts of strong targets and weak targets. It can significantly improve the detection rate of infrared small targets while ensuring a small change in the false alarm rate and segmentation accuracy, thus improving the overall performance of the model.

In summary, we propose an innovative infrared small target detection scheme based on an adjustable sensitivity strategy and multi-scale fusion. On the basis of this scheme, we win the first prize in the PRCV 2024 wide-area infrared small target detection. The contributions of this manuscript can be summarized as follows:

- (1) To solve the problem of large differences in image resolution and target scale, on the one hand, we explore multiple excellent infrared small target detection networks and select MSDA-Net as our backbone network. On the other hand, we propose a multi-scale fusion strategy, which helps to extract effective features of targets at different scales.

- (2) We propose an edge enhancement difficulty mining loss, which can guide the network to pay more attention to difficult target regions and edge features during training, thereby promoting positive network optimization

(3) We propose an adjustable sensitivity strategy for post-processing. This strategy is conducive to significantly improving the detection rate of infrared small targets while ensuring a small change in the false alarm rate and segmentation accuracy.

2 Related Work

2.1 Non-deep learning-based infrared small target detection methods

Early non-deep learning-based infrared small target detection methods regard infrared small targets as protrusions in the background and use spatial domain filtering and transform domain filtering. The spatial domain filtering methods include Max-Median filter[9] and two-dimensional minimum mean square error filter[10]. The transform domain filtering methods include dual-tree complex wavelet, dual-tree complex wavelet, and discrete cosine transform (DCT) [11]. Subsequently, researchers propose the human visual system-based methods and image data structure-based methods to further improve the performance of non-deep learning-based infrared small target detection methods. Representative works based on the human visual system include the local contrast measure (LCM) [2] and multi-scale patch-based contrast measure (MPCM) [3]. Representative works based on image data structure methods include the infrared patch-image model (IPI) [4] and the non-negative infrared patch-image model based on partial sum minimization of singular values (NIPPS) [12]. However, for highly complex actual scenes, such as images containing background edges and high-brightness noise points that have local features similar to those of small targets, the above non-deep learning-based methods are prone to false detection.

2.2 Deep learning-based infrared small target detection methods

Different from non-deep learning-based methods, deep learning-based methods learn the features of infrared small targets in a data-driven manner. In the early days, Liu et al. [13] propose the first SIRST detection method based on deep learning. They design a 5-layer multi-layer perception network for infrared small target detection. Subsequently, more and more researchers began to explore deep learning-based infrared small target detection methods. Specifically, Dai et al. propose the asymmetric context module [14] and the attention local contrast network (ALCNet) [15]. Subsequently, Yu et al. propose a multi-scale local contrast learning network (MLCL-Net) [16] and an attention-based local contrast learning network (ALCL-Net) [5] to further strengthen the extraction of the relationships among local features. Recently, Li et al. propose a densely nested attention network (DNANet) [6], which uses UNet++ as the basic structure and performs repeated feature fusion and enhancement through densely nested interaction modules and channel space attention modules. At the same time, Wu et al. propose a U-Net nested network (UIU-Net) [17] to achieve multi-scale feature fusion. Subsequently, Zhao et al. further emphasize the gradient information and directional characteristics of infrared small target images and propose GGL-Net [7] and MSDA-Net [8] respectively. In addition, Zhang et al. propose an infrared shape network (ISNet) [18] to enhance the feature extraction

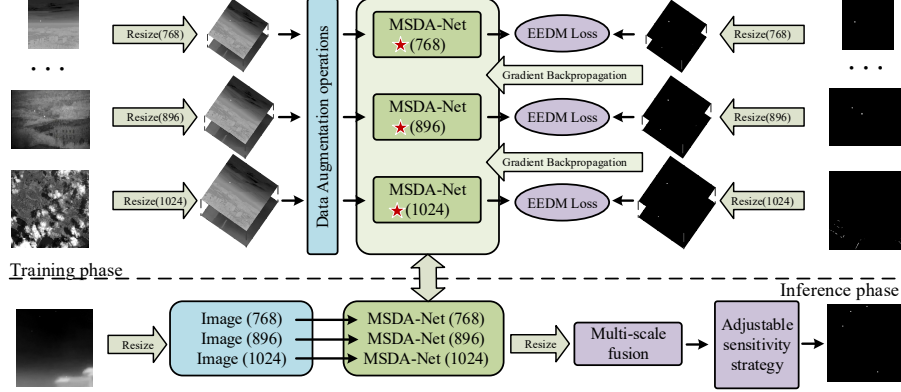


Fig. 1. Structure of the overall scheme

capability of the network by extracting the target shape. However, existing deep learning-based infrared small target detection methods are often optimized for a fixed image resolution, a single wavelength, or a specific imaging system, limiting their breadth and flexibility in practical applications. Therefore, we aim to build a wide-area infrared small target detection scheme with strong generalizability and high detection accuracy.

3 Methods

3.1 Overall scheme introduction

From Fig. 1, the proposed scheme consists of two parts: a model training phase and a model inference phase. In the model training phase, we adopt the MSDA-Net proposed in our previous work [8] as the backbone model. MSDA-Net mainly emphasizes the attention to high-frequency directional features in images, thereby promoting the refined extraction of infrared small target features. First, the training images are resized to 768×768 , 896×896 , and 1024×1024 and then input into the models of the corresponding sizes for training. This operation is beneficial for improving the network's generalization ability for data of different scales. Secondly, to further improve the detection accuracy, we use the proposed EEDM loss. In the model inference phase, first, the prediction results of multiple scale models are fused. Multi-model fusion is beneficial for improving the network's detection performance for multi-scale images while reducing the false alarm rate. Then, the fused results are post-processed using the proposed AS strategy. The use of the AS strategy is beneficial for greatly improving the detection rate.

3.2 Adjustable sensitivity strategy

In the infrared small target detection task, the network outputs a probability mask map, in which the value of each point denotes the confidence that the point is the

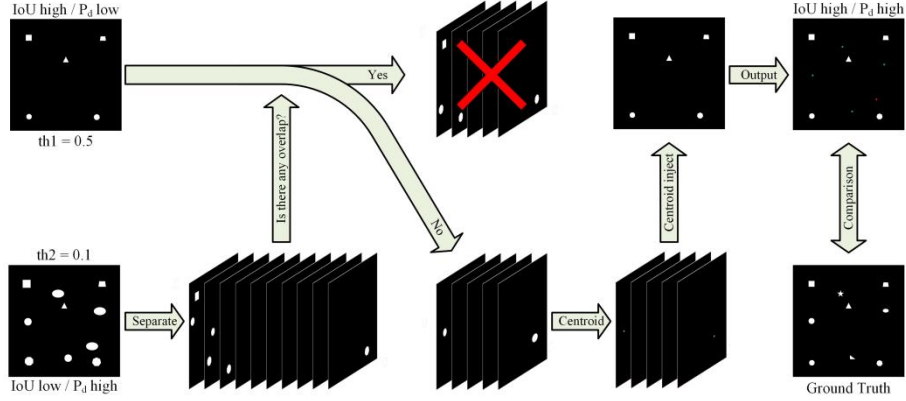


Fig. 2. Adjustable sensitivity strategy.

target. Existing methods generally use areas with a threshold greater than 0.5 as the target area. However, considering the complexity and diversity of real-world application scenarios, how to implement an intelligent detection strategy with a higher detection rate and stronger generalizability is a very challenging task. To solve this problem, we propose an AS strategy. Regarding the probability mask map output by the network and its practical application, we define the concepts of strong targets and weak targets. Existing deep learning networks already have powerful feature extraction capabilities. A strong target is one that is obvious and can be detected by the network. A weak target is one that is difficult to detect and it is difficult to determine whether it is a target area. For strong targets, we aim to segment them completely and finely. For weak targets, we aim to detect them (in point form) to meet the needs of some scenarios. Notably, through many experimental observations and analyses, when the network performance is not extremely poor, the predicted values of most simple backgrounds in the prediction results are infinitely close to 0. Even if the threshold is very small, the final segmentation result will not release many messy areas.

From Fig. 2, for the output probability mask map, we introduce two thresholds, namely, $th1$ (0.5) and $th2$ (0.1). The area where the threshold is greater than $th1$ is identified as a strong target area. The area where the threshold is between $th2$ and $th1$ is a weak target area. For the probability mask map using only a single threshold, gradually reducing the threshold will evolve more target areas in the original segmentation map. However, directly using $th2$ (0.1) will result in many false positives. Therefore, the AS strategy we propose solves this problem. First, we separate the segmentation result M_{th2} of $th2$ (0.1) into multiple binary images $M_{th2}^s, s = 1, 2, \dots, n$ with a single target area according to a single connected region. Secondly, these binary images $M_{th2}^s, s = 1, 2, \dots, n$ are compared with the segmentation results M_{th1} of $th1$ (0.5) in turn to determine whether there are overlapping areas. For M_{th2}^s with overlapping areas, we lose it. For the same target area, the fineness in M_{th1} is better than that in M_{th2} . Thirdly, we extract the centroid of M_{th2}^s where there is no

overlapping area. Finally, the extracted centroid points are injected into M_{th1} to generate the final segmentation result map. The highlighted weak target area is added to M_{th1} in the form of centroid points without affecting the fine segmentation of the strong target area in M_{th1} .

3.3 Multi-scale fusion strategy

Since using a single network model for detection affects the network's detection performance for multi-scale infrared small targets and multi-size samples, we propose a multi-scale fusion strategy. Specifically, we resize the images to 768×768 , 896×896 , and 1024×1024 and input them into the corresponding networks to generate models of corresponding sizes. The test images are then resized to 768×768 , 896×896 , and 1024×1024 and input into the trained model for inference. Finally, the inference results are restored to the original image size and fused.

Fusing models at multiple scales helps to characterize features such as the shape, edge, and texture of targets at different scales, making the model more accurate and reliable in identifying and locating targets. In addition, real detection scenarios are often more complex and changeable, so fusing models of different scales can help improve the robustness of the model in complex backgrounds and at different resolutions.

3.4 Edge enhancement difficulty mining loss

In the task of infrared small target detection, the small target area and lack of intrinsic features make it difficult to accurately locate in the image. Therefore, on the basis of the characteristics of infrared small targets, we design an EEDM loss. This loss helps alleviate the problem of class imbalance and guides the network to pay more attention to difficult samples and marginal features during training.

Specifically, the EEDM loss first extracts the edge contour of the infrared small target from the true label to obtain the edge map e . At the same time, an edge weight w is set, and the edge map e is weighted using w to obtain the edge weight matrix e' . Considering that infrared small targets are usually small and inconspicuous, edge weighting w can effectively enhance the response of the target edge, making small targets more conspicuous in detection. The formula is as follows:

$$e' = \begin{cases} 1 & \text{if } e = 0 \\ w & \text{if } e > 0 \end{cases} \quad (1)$$

Secondly, the loss value matrix L_{BCE} of each pixel point is used by the binary cross-entropy loss, and the edge weighting matrix e' is used to weight L_{BCE} to obtain the weighted loss value L^* . The formula is as follows:

$$L_{BCE} = y_i \log(\hat{y}_i) + (1 - y_i) \log(1 - \hat{y}_i) \quad (2)$$

$$L^* = e' \times L_{BCE} \quad (3)$$

where y_i denotes the true label of the i -th pixel, and \hat{y}_i denotes the probability of the i -th pixel being predicted as the target.

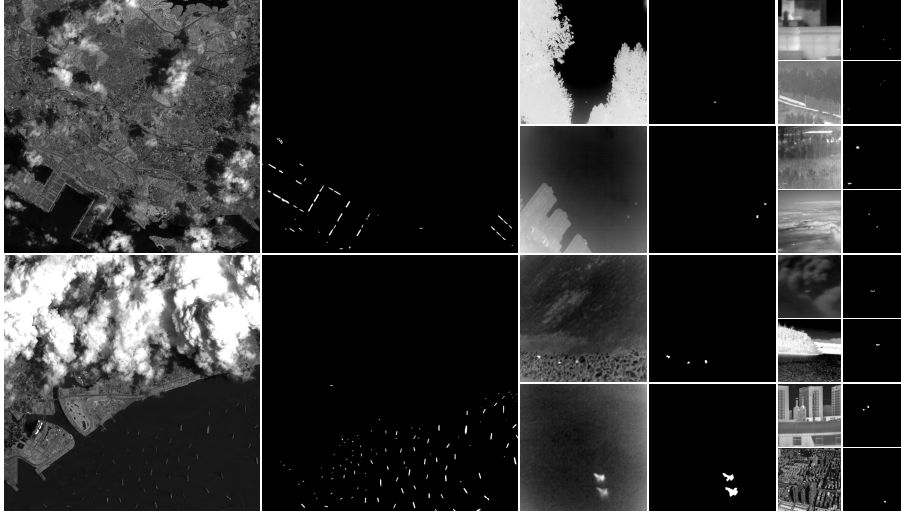


Fig. 3. Some samples from the W-IRSTD dataset and their true labels.

Thirdly, the difficulty value mining is performed on the edge weighted loss value matrix L^* . The specific steps of difficult value mining are to sort the loss values of the total number of pixel points N , and then select a set whose loss value is greater than or equal to the median position loss value. The formula is as follows:

$$L_{sorted} = sort(L^*) \quad (4)$$

$$L_{hard} = \{L_i | L_i \geq L_{sorted}[\lfloor 0.5 \times N \rfloor]\} \quad (5)$$

Finally, the average loss of the difficulty value is calculated to obtain the final loss. The formula is as follows:

$$L_{EEDM} = \frac{1}{|L_{hard}|} \sum_{i \in L_{hard}} L_{hard}[i] \quad (6)$$

EEDM loss uses edge information as an additional constraint, driving the network to pay more attention to edge features during training. For infrared small target detection tasks, the target is usually small and inconspicuous. By emphasizing the edge, the response of the target edge can be effectively enhanced, making the small target more conspicuous in detection. At the same time, the loss function adopts a difficulty mining strategy, which helps the model learn important features more effectively instead of being overwhelmed by a large number of simple background areas.

4 Experiments

4.1 Dataset

We use the dataset given in the PRCV 2024 wide-area infrared small target detection competition. The dataset contains 9,000 images, mainly from seven public

datasets: SIRST-V2, IRSTD-1K, IRDST, NUDT-SIRST, NUDT-SIRST-sea, NUDT-MIRSDT and Anti-UAV410. The images contained in this dataset come from multiple observation perspectives (land-based, air-based, and space-based), cover a variety of target types (extended targets, spot targets, and point targets), and use multiple bands (shortwave, longwave, and near-infrared) and multiple resolutions (256×256 , 512×512 , and 1024×1024 , etc.). For convenience of description and considering its characteristics, we call the dataset we are studying the wide-area infrared small target detection (W-IRSTD) dataset. Fig. 3 shows some samples from the W-IRSTD dataset. There are clearly significant differences between the samples, and the target types are rich. In the experiments, we randomly divide 9000 images into training and test sets at a 4:1 ratio.

4.2 Experimental settings

1) *Experimental environment and parameter settings.* The experimental environment is an Ubuntu 18.04 operating system, and the GPU is an RTX 3090 24 GB. The training epoch, batch size, and learning rate are 300, 10, and $5e-4$, respectively.

2) *Evaluation metrics.* The scoring metrics we use are consistent with those in the PRCV 2024 wide-area infrared small target detection competition. Specifically, we use pixel-level metrics (intersection over union (IoU)) and object-level metrics (detection rate P_d and false alarm rate F_a) to evaluate the performance of the model [6]. The final comprehensive evaluation metric *Score* is calculated by the IoU and P_d under a certain F_a constraint. The *Score* can be used to comprehensively evaluate the region segmentation accuracy and target detection accuracy of the model. The formula is as follows:

$$Score = \alpha \times IoU + (1 - \alpha) \times P_d \quad (7)$$

where $\alpha = 0.5$. In addition, F_a has a constraint effect. When F_a is less than $1e^{-4}$, the final result is considered valid.

4.3 The selection of backbone networks

To achieve precise infrared small target detection, we explore several excellent infrared small target detection methods. To compare the performance of each method more fairly and select the method with the best performance as the backbone network, we reproduce each method under a unified framework. We use the proposed EEDM loss and uniformly adjust the input image to 512×512 pixels for input. The experimental results are shown in Table 1.

From Table 1, MSDA-Net achieves better results in terms of both segmentation accuracy and detection accuracy. Specifically, compared with DNANet [6], GGL-Net [7], and UIU-Net [17], MSDA-Net improves the performance of the IoU and P_d by 1.52 - 2.23 and 1.15 - 2.78, respectively. At the same time, compared with the final scores of other networks, MSDA-Net can improve 1.64 - 20.58. Of course, it can also be seen from the results that the false alarm rate of MSDA-Net is relatively high. However, compared with constraint ($1e^{-4}$), this false alarm rate is completely acceptable.

Table 1. Performance comparison of various excellent methods on the W-IRSTD dataset.

Methods	IoU	nIoU	P _d	F _a ($\times 10^{-6}$)	Param	Scores
ACM ^[14]	40.61	27.91	38.86	7.34	0.398	39.74
ALCNet ^[15]	43.55	29.43	40.49	7.04	0.427	42.02
MLCL-Net ^[16]	53.28	33.37	59.38	9.16	0.560	56.33
ALCL-Net ^[5]	53.36	34.21	60.51	9.17	5.668	56.94
DNANet ^[6]	55.08	34.69	60.56	8.41	4.697	57.82
GGL-Net ^[7]	55.07	34.82	62.19	10.09	8.988	58.63
UIU-Net ^[17]	55.78	35.04	61.58	13.64	50.541	58.68
MSDA-Net ^[8]	57.30	35.72	63.34	14.25	4.791	60.32

Table 2. Performance comparison of different losses on the W-IRSTD dataset.

Scheme	IoU	nIoU	P _d	F _a ($\times 10^{-6}$)	Scores
BCE Loss	54.05	34.38	59.49	8.87	56.77
Dice Loss	50.15	35.35	60.09	9.09	55.12
Edge Enhancement Loss	56.26	34.44	60.46	8.51	58.36
EEDM Loss	57.30	35.72	63.34	14.25	60.32

4.4 Effect verification of the EEDM loss

To further verify the effect of the proposed EEDM loss, we conduct a detailed experimental exploration. Notably, we also study SoftIoU loss, but the network is difficult to train on the W-IRSTD dataset, so we do not compare it. In the experiment, all the data are adjusted to 512×512 pixels as input, and the model is MSDA-Net. From Table 2, compared with the BCE loss and Dice loss, the proposed EEDM loss results in more obvious increases in the IoU and P_d, which verifies the superiority of EEDM loss for infrared small target detection tasks.

4.5 Effect verification of the multi-scale model fusion

From Tables 1 and 2, we select MSDA-Net as the backbone model and use EEDM loss as the loss function. However, considering the large size differences of infrared small target images in practical applications, the detection performance of multiple resolutions using only a single-scale model is limited. Therefore, we propose to use multi-scale model fusion. We explore the differences in model performance for different sizes (256, 384, 512, 640, 768, 896, 1024). The image patches are of the same length and width.

From Table 3, the 1024 model achieves the best performance. Compared with the worst-performing 256 model, the 1024 model improves the IoU, P_d, and Scores by 16.35, 27.42, and 21.88, respectively. For the W-IRSTD dataset, if the image is adjusted to a smaller size and input into the network, such as 256×256 , the model performance decreases significantly. The reason is that during the image reduction process, the number of pixels of small targets decreases or even disappears

Table 3. Performance comparison of models of different scales on the W-IRSTD dataset.

Scheme	IoU	nIoU	P _d	F _a ($\times 10^{-6}$)	Scores
256	43.78	30.03	48.75	13.79	46.27
384	53.79	34.02	64.89	11.19	59.34
512	57.30	35.72	63.34	14.25	60.32
640	59.65	37.06	72.05	11.55	65.85
768	60.67	37.45	70.90	13.53	65.79
896	61.89	36.73	71.95	12.32	66.92
1024	60.13	38.22	76.17	12.78	68.15

Table 4. Comparison of the fusion performance of multi-scale models on the W-IRSTD dataset

Scheme	IoU	nIoU	P _d	F _a ($\times 10^{-6}$)	Scores
896	61.89	36.73	71.95	12.32	66.92
896+768	63.12	37.74	70.85	9.32	66.99
896+768+1024	64.49	38.38	72.61	9.17	68.55
896+768+1024+640	64.11	38.34	72.42	7.96	68.27
896+768+1024+640+512	63.60	38.06	70.43	7.25	67.02
896+768+1024+640+512+384	62.83	37.54	68.72	6.75	65.78
896+768+1024+640+512+384+256	61.44	36.69	65.94	6.17	63.69

completely, which makes it difficult for the network to extract effective target features. At the same time, considering that the proposed AS strategy will be used in the future, it is mainly aimed at improving the detection rate of the model. Therefore, to ensure accurate segmentation, we select the 896 model with the best IoU as the basis and fuse the scale models with the suboptimal IoU one by one. The experimental results are shown in Table 4.

From Table 4, we can see that fusing the 896 model, the 768 model, and the 1024 model results in the greatest performance improvement. Specifically, compared with the 896 model, which has the best performance at a single scale, the fusion of the 896 model, the 768 model and the 1024 model can improve its IoU, P_d and *Score* by 2.60, 0.66 and 1.63, respectively. At the same time, we find that when the performance of the fused scale models degrades severely, it will lead to the degradation of the performance of the final model. In addition, the multi-scale fusion model will perform better on F_a, which shows that the multi-scale model fusion strategy is conducive to reducing the missed detections and further improving the reliability of the model. To more intuitively demonstrate the effect of multi-scale model fusion, we show the prediction results of the 896 model, 768 model, 1024 model and their fusion model in Fig. 4.

4.6 Effect verification of the adjustable sensitivity strategy

To further verify the AS strategy, we adjust the thresholds th1 and th2 on the optimal multi-model fusion scheme (896+768+1024). Table 5 shows the experimental

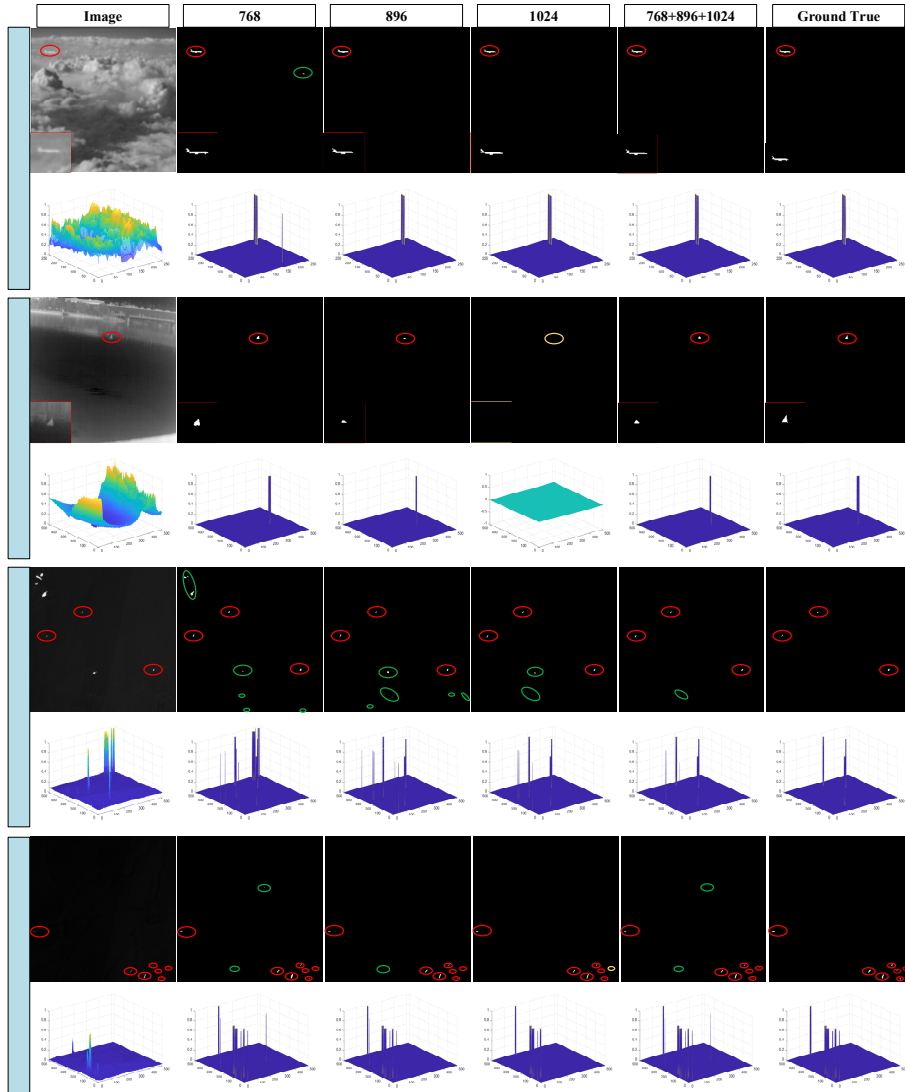


Fig. 4. Detection results of the fusion model and its corresponding single model. Red circles denote correct detections, green circles denote false detections, and yellow circles denote missed detections.

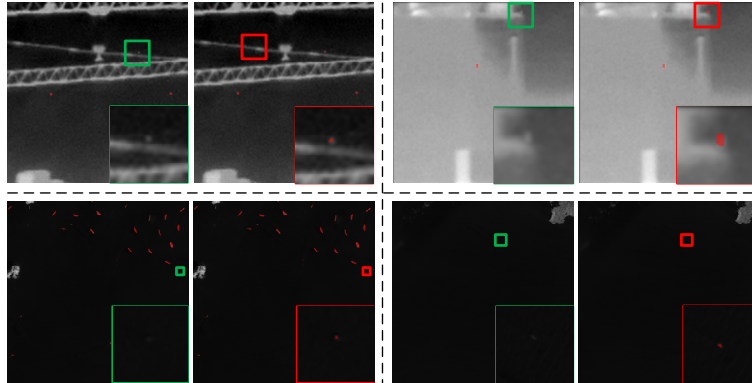
results obtained by adjusting the threshold th_1 alone without adjusting the threshold th_2 . Table 6 shows the experimental results obtained by adjusting the threshold th_2 on the basis that th_1 is set to the optimal value in Table 5. From Table 5, when the threshold th_1 decreases from 0.5 to 0.3, the best overall performance can be achieved. Specifically, compared with setting the threshold th_1 to 0.5 in the usual case, the comprehensive evaluation *Scores* are increased by 5.41% (from 68.55 to 72.26) when th_1 is set to 0.3. The detection rate P_d increased by 10.58% (from 72.61 to 80.29).

Table 5. Performance comparison of adjusting the threshold th1 on the W-IRSTD dataset.

Scheme	th1	IoU	nIoU	P _d	F _a ($\times 10^{-6}$)	Scores
896+768+1024 (0.5)	0.5	64.49	38.38	72.61	9.17	68.55
896+768+1024 (0.45)	0.45	65.53	39.33	74.86	10.51	70.20
896+768+1024 (0.4)	0.4	65.91	40.09	76.44	13.03	71.18
896+768+1024 (0.35)	0.35	65.58	40.48	78.56	15.67	72.07
896+768+1024 (0.3)	0.3	64.22	40.41	80.29	20.57	72.26
896+768+1024 (0.25)	0.25	61.83	39.86	82.34	26.85	72.09
896+768+1024 (0.2)	0.2	58.34	38.83	83.91	35.93	71.13
896+768+1024 (0.15)	0.15	53.43	37.40	85.28	50.52	69.36
896+768+1024 (0.1)	0.1	46.27	34.83	86.43	76.12	66.35
896+768+1024 (0.05)	0.05	35.15	30.56	87.72	138.46	-

Table 6. Performance comparison of adjusting the threshold th2 on the W-IRSTD dataset.

Scheme	th1	th2	IoU	nIoU	P _d	F _a ($\times 10^{-6}$)	Scores
896+768+1024 (0.3)	-	-	64.22	40.41	80.29	20.57	72.26
896+768+1024 (0.3+0.5)	-	0.5	63.96	40.23	81.61	21.26	72.79
896+768+1024 (0.3+0.4)	-	0.4	63.78	40.14	83.02	21.76	73.40
896+768+1024 (0.3+0.3)	0.3	0.3	63.45	40.01	85.28	22.66	74.37
896+768+1024 (0.3+0.2)	-	0.2	62.81	39.74	87.51	24.29	75.16
896+768+1024 (0.3+0.1)	-	0.1	61.42	39.23	89.98	28.11	75.70
896+768+1024 (0.3+0.05)	-	0.05	59.44	38.48	91.05	33.05	75.25

**Fig. 5.** Comparison of AS strategy effects. The left and right sides of each set of data are the results without and with the AS strategy, respectively. The green box denotes a local detection error, and the red box denotes a local detection correctness.

Notably, when the threshold th1 is reduced to 0.05, F_a will surge and exceed the constraint range.

From the experimental results in Table 6, it can be seen that the introduction of threshold th_2 can significantly improve the performance of the model. For example, when th_1 is 0.3 and th_2 is 0.1, the *Scores* can be improved by 4.76% (from 72.26 to 75.70) over the result of using only th_1 equal to 0.3. At the same time, compared with the results in Table 2, it can be seen that the introduction of threshold th_2 greatly improves the detection rate while ensuring the accuracy of infrared small target segmentation and reasonably controlling the false alarm rate. To more intuitively demonstrate the effectiveness of the AS strategy, we present some results as shown in Fig. 5.

It is worth mentioning that in the PRCV 2024 wide-area infrared small target detection competition, the final solution we choose is "384+512+640+768+896" as the multi-scale fusion model, and th_1 and th_2 are 0.35 and 0.1, respectively.

5 Conclusion

This manuscript proposes a refined infrared small target detection scheme based on an adjustable sensitivity strategy and multi-scale fusion, which constructs a wide-area infrared small target detection architecture with strong generalizability and high detection accuracy. To solve the problem of large differences in image resolution and target scale, we adopt a multi-scale fusion strategy based on the selected backbone network MSDA-Net. The fusion of multi-scale models helps make the model more accurate and reliable in identifying and locating targets. At the same time, to alleviate the problem of class imbalance and guide the network to pay more attention to difficult samples and edge features during training, we propose an EEDM loss. This loss helps the model to effectively learn more valuable features, greatly avoiding the risk of small targets being overwhelmed by a large number of background features. Finally, to further improve the overall performance, we propose an AS strategy for post-processing, which is beneficial for significantly improving the detection rate of infrared small targets while ensuring the accuracy of model segmentation. Extensive experimental results show that the proposed scheme achieves outstanding comprehensive performance in infrared small target detection.

References:

- [1] Huang, B., Li, J., Chen, J., Wang, G., Zhao, J. Xu, T.: Anti-uav410: A thermal infrared benchmark and customized scheme for tracking drones in the wild. *IEEE Transactions on Pattern Analysis and Machine Intelligence* **46**(5), 2852-2865 (2023)
- [2] Chen, C., Li, H., Wei, Y., Xia, T., Tang, Y.: A local contrast method for small infrared target detection. *IEEE Transactions on Geoscience and Remote Sensing* **52**(1), 574-581 (2014)
- [3] Wei, Y., You, X., Li, H.: Multiscale Patch-Based Contrast Measure for Small Infrared Target Detection. *Pattern Recognition* **58**, 216-226 (2016)
- [4] Gao, C., Meng, D., Yang, Y., Wang, Y., Zhou, X., Hauptmann A.: Infrared patch-image model for small target detection in a single image. *IEEE Transactions on Image Processing* **22**(12), 4996-5009 (2013)

- [5] Yu, C., Liu, Y., Wu, S., Xia, X., Hu, Z., Lan, D., Liu, X.: Pay Attention to Local Contrast Learning Networks for Infrared Small Target Detection. *IEEE Geoscience and Remote Sensing Letters*, **19**, 1-5 (2022)
- [6] Li, B., Xiao, C., Wang, L., Wang, Y., Lin, Z., Li, M., An, W., Guo, Y.: Dense nested attention network for infrared small target detection. *IEEE Transactions on Image Processing* **32**, 1745-1758 (2023)
- [7] Zhao, J., Yu, C., Shi, Z., Liu, Y., Zhang, Y.: Gradient-Guided Learning Network for Infrared Small Target Detection. *IEEE Geoscience and Remote Sensing Letters* **20**, 1-5 (2023)
- [8] Zhao, J., Lin, Z., Yu, C., Liu, Y.: Multi-Scale Direction-Aware Network for Infrared Small Target Detection. *ArXiv Preprint*, arXiv:2406.02037.
- [9] Arce, G., McLoughlin, M.: Theoretical Analysis of the Max/Median Filter. *IEEE Transactions on Acoustics, Speech, and Signal Processing* **35**(1), 60–69 (1987)
- [10] Zhao, Y., Pan, H., Du, C., Peng, Y., Zheng, Y.: Two-Dimensional Least Mean Square Filter for Infrared Small Target Detection. *Infrared Physics & Technology* **65**, 17–23 (2014)
- [11] Chouhan, R., Biswas, P., Jha, R.: Enhancement of low-contrast images by internal noise-induced Fourier coefficient rooting. *Signal, Image and Video Processing* **9**, 255-263 (2015)
- [12] Dai, Y., Wu, Y., Song, Y., Guo, J.: Non-negative infrared patch-image model: Robust target-background separation via partial sum minimization of singular values. *Infrared Physics & Technology* **81**, 182-194 (2017)
- [13] Lin, L., Wang, S., Tang, Z.: Using deep learning to detect small targets in infrared oversampling images. *Journal of Systems Engineering and Electronics* **29**(5), 947-952 (2018)
- [14] Dai, Y., Wu, Y., Zhou, F., Barnard K.: Asymmetric Contextual Modulation for Infrared Small Target Detection. In: *WACV*. pp. 950-959 (2021)
- [15] Dai, Y., Wu, Y., Zhou, F., Barnard, K.: Attentional Local Contrast Networks for Infrared Small Target Detection. *IEEE Transactions on Geoscience and Remote Sensing* **59**(11), 9813-9824 (2021)
- [16] Yu, C., Liu, Y., Wu, S., Hu, Z., Xia, X., Lan, D., Liu, X., Infrared small target detection based on multiscale local contrast learning networks. *Infrared Physics & Technology* **123**, (2022)
- [17] Wu, X., Hong, D., Chanussot, J.: UIU-Net: U-Net in U-Net for infrared small object detection. *IEEE Transactions on Image Processing*, **32**, 364-376 (2023)
- [18] Zhang, M., Zhang, R., Yang, Y., Bai, H., Zhang, J., Guo, J.: ISNet: Shape matters for infrared small target detection. In: *CVPR*. pp. 877-886 (2022)